Boundary interaction of the Vicsek model and its hydrodynamic model

Hui Yu

Institut für Geometrie und Praktische Mathematik
RWTH Aachen University, Germany

Joint work with Dieter Armbruster and Michael Herty.

KI-Net Conference on Kinetic Descriptions of Chemical and
Biological Systems: Models, Analysis and Numerics
Iowa State University
March 23, 2017

Figure: Collective motion. No external signal or leadership.

(a) Fish school.　　(b) Herds of caribou.

Applications: cell motion, fish farming, pedestrian flow, ...

The descriptions in three scales:

- Microscopic: Individual-Based Models (IBM).

  I. Aoki, H. Chaté, F. Ginelli, A. Czirok, T. Vicsek, ...

- Mesoscopic: Kinetic Models.

  N. Bellomo, J. Soler, E. Bertin, J. A. Carrillo, ...

- Macroscopic: Fluid Models.

  A. L. Bertozzi, J. Toner, Y. Tu, P. Degond, J.-G. Liu, ...

▶ The size of system is larger than the interaction range between individuals by several order of magnitude.

▶ The large-scale structures are of great interest.

▶ Hydrodynamic limit.

The Vicsek Individual-Based Model

For a system of N particles in the space $\mathbb{R}^n$, each of them is described by its position $X_k(t)$ and the direction $\omega_k \in \mathbb{S}^n$:

$$
\begin{cases}
\dfrac{dX_k}{dt} = v_k, \\
v_k = v_0 \omega_k - \mu \nabla_{\boldsymbol{x}} \Phi(X_k(t)), \\
d\omega_k = \mathcal{P}_{\omega_k^\perp}(\nu \bar{\omega}_k dt + \alpha v_k dt + \sqrt{2D} dB_t).
\end{cases}
$$
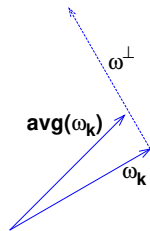
where v_0, ν, α and D are positive constant parameters, and

$$
\bar{\omega}_k = \frac{J_k}{|J_k|} \quad \text{with } J_k = \sum_{i=1}^{N} K(|X_i - X_k|)\omega_i.
$$

Ref.: T. Vicsek, A. Czirók, E. Ben-Jacob, I. Cohen and O. Shochet (1995).

μ is the repulsion frequency for the volumn exclusion and $\Phi(\boldsymbol{x})$ is the repulsion potential, defined by

$$\Phi(\boldsymbol{x}) = \frac{1}{N\varepsilon^2} \sum_{1 \leq i \leq N} \phi\left(\frac{|\boldsymbol{x} - X_i|}{r}\right),$$

where $r > 0$ is the interaction range for the repulsion force between particles and ε is in the same order as $\frac{1}{\nu}$. Note that $\Phi(\boldsymbol{x})$ approaches ∞ as $\boldsymbol{x} \to X_i$. We consider an experimental choice of $\phi(|z|)$ for $z \in \mathbb{R}^2$:

$$\phi(|z|) = \left\{ \begin{array}{ll} (|z| - 1)^2, & \text{if } |z| \leq 1; \\ 0, & \text{elsewhere}. \end{array} \right.$$
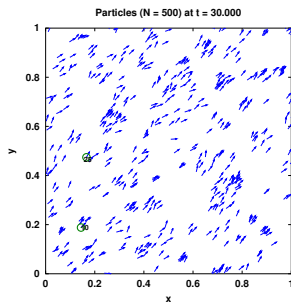
Two commen choices are:

- Periodic boundary condition.

- Reflection at the boundary.

Leading to alignment associated with uniform density distribution.
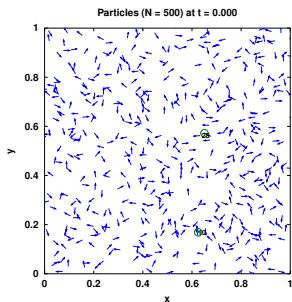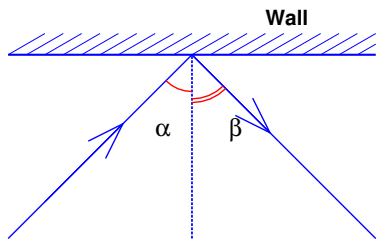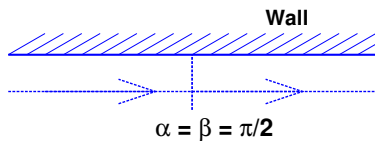

(c) Random data at $t = 0$ (d) $t = 30$

Figure: Periodic boundary condition.

(a) (b)

Figure: Symmetric reflection with respect to the normal direction at the boundary. α: incoming angle. β: outgoing angle.

Remark: The particles travelling along the boundary will maintain the orientation parallel to the wall.

- The experiments are performed by Plouraboué, et al., Institut de Mécanique des Fluides de Toulouse.
- The annular domain in 2D: $\{x \in \mathbb{R}^2 : R_1 \leq |x| \leq R_2\}$.
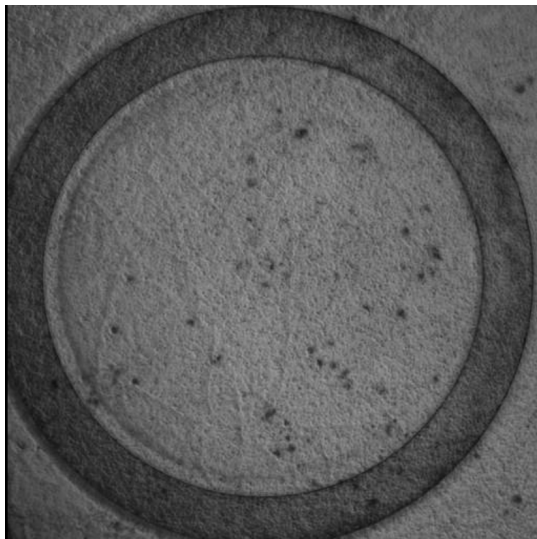
- The particles display a rotational collective motion in time.

- One can observe high concentration near the boundary.

- The particles nearby the boundary linger awhile and slowly drift away.

- Besides the repulsion enforced by the wall, the particle also interact with its neighbors.
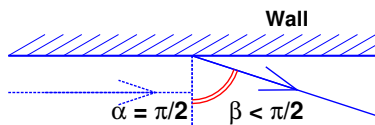
  Particularly, the particles in the front of a swarming body experience the alignment to the average orientation due to the particles following behind.

- The particles have the tendency moving away from the boundary.

Remark: It is close to reality to consider asymmetric reflection, or soft reflection.
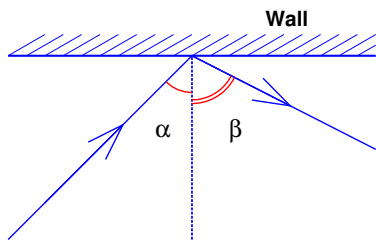
(a)   (b)

Figure: Soft reflection with respect to the normal direction at the boundary. α: incoming angle. β: outgoing angle.

For the particles interaction with the boundary, we apply the soft reflection in the following way.

1. The new location is reflected to the inside w.r.t. the boundary.

For the particles interaction with the boundary, we apply the soft reflection in the following way.

1. The new location is reflected to the inside w.r.t. the boundary.
2. The new orientation is the result of the symmetric reflection and the alignment to the average orientation.

$$d\omega_k = \mathcal{P}_{\omega_k^\perp}(\sigma\bar{\omega}_k dt + \sqrt{2D_b}dB_t).$$

σ and D_b are the alignment frequency and the noise due to the Brownian motion, respectively.

They can be different from ν and D inside of the domain. One experimental choise is that $\sigma >= \nu$ and $D_b \approx D$ due to the compactness nearby the boundary.

Consider the discrete setting in time for

$$d\omega_k = \mathcal{P}_{\omega_k^\perp}(\sigma\bar{\omega}_k dt + \sqrt{2D_b}dB_t).$$

$\bar{\omega}_k$ is taken at the previous time step, say t^n. Then this equation gives the outgoing orientation ω^{n+1}.

However, due to the presence of the Brownian motion in the individual-based model, particles will move away from the boundary.

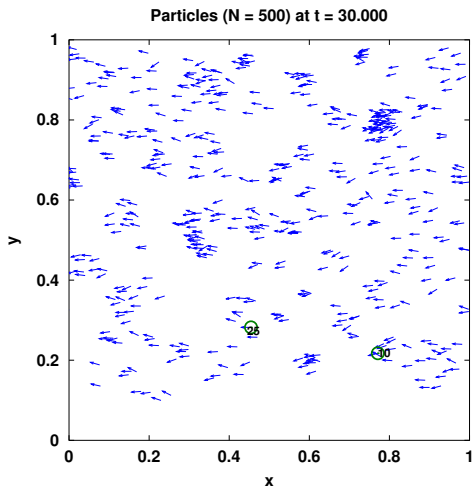So there is no significant difference by applying symmetric and soft reflection.

Figure: Periodic in *x* and symmetric reflection in *y*. The particles move to the left and bounce up and down in the verticle direction.

For the deterministic hydrodynamci model, different boundary behavior will be induced by the soft reflection.

We extract the new reflection law using the particle model.

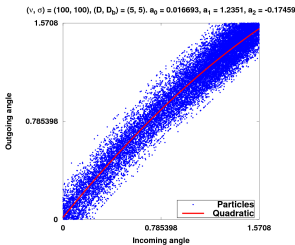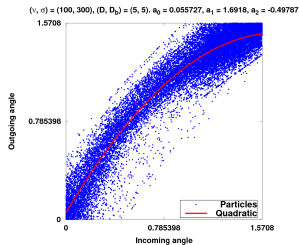1. Start with a self-orgazied swarming body in a confined square such that sufficient boundary interactions happen.

Particles (N = 1000) at t = 0.000
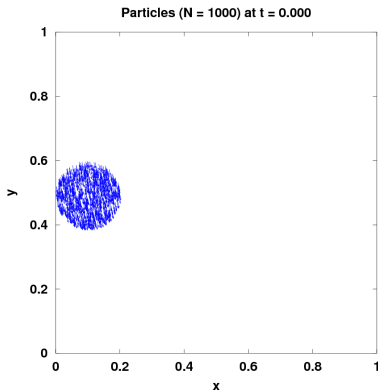
New reflection law

For the determined hydrodynamci model, one will expect different behavior induced by the soft reflection.

We extract the new reflection law using the particle model.

1. Start with a self-orgazied swarming body in a confined square such that sufficient boundary interactions happen.

2. Record all the incoming and outgoing angles for each particle hitting the boundary.

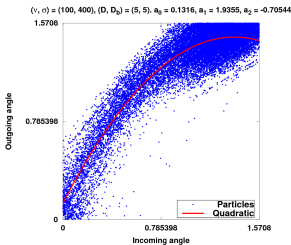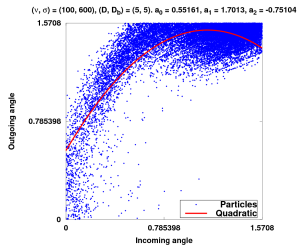3. The parameter fitting shows a quadratic law between the incoming and outgoing angles.

(a) $\sigma = 100$.

(b) $\sigma = 300$.

(c) $\sigma = 400$.

(d) $\sigma = 600$.

YU, Hui · Boundary interaction for collection motion

The SOHR model

The Self-Organized Hydrodynamic model is given below:

$$\begin{cases} \partial_t \rho + c_1 \nabla \cdot (\rho U) = 0, \\ \rho\left[\partial_t \Omega + c_2 (V \cdot \nabla)\Omega\right] + d\mathcal{P}_{\Omega^\perp}\nabla\rho = \gamma\mathcal{P}_{\Omega^\perp}\Delta(\rho\Omega), \\ |\Omega| = 1, \end{cases}$$

where

$$U = c_1 v_0 \Omega - \mu\Phi_0 \nabla_{\boldsymbol{x}}\rho, \quad V = c_2 v_0 \Omega - \mu\Phi_0 \nabla_{\boldsymbol{x}}\rho,$$

$$p(\rho) = dv_0\rho + \alpha\mu\Phi_0(d + c_2)\frac{\rho^2}{2}, \quad \gamma = k_0(d + c_2)\frac{v_0^2}{\nu}.$$

Compared to the isothermal compressible Navier-Stokes equation,

- $c_1 \neq c_2$ due to the lack of Galilean invariance;
- Instead of momentum conservation, there is the geometric constraint on Ω.

The Self-Organized Hydrodynamic model is given below:

$$\begin{cases} \partial_t \rho + c_1 \nabla \cdot (\rho U) = 0, \\ \rho \left[\partial_t \Omega + c_2 (V \cdot \nabla) \Omega \right] + d \mathcal{P}_{\Omega^\perp} \nabla \rho = \gamma \mathcal{P}_{\Omega^\perp} \Delta (\rho \Omega), \\ |\Omega| = 1, \end{cases}$$

where

$$U = c_1 v_0 \Omega - \mu \Phi_0 \nabla_{\boldsymbol{x}} \rho, \quad V = c_2 v_0 \Omega - \mu \Phi_0 \nabla_{\boldsymbol{x}} \rho,$$

$$p(\rho) = d v_0 \rho + \alpha \mu \Phi_0 (d + c_2) \frac{\rho^2}{2}, \quad \gamma = k_0 (d + c_2) \frac{v_0^2}{\nu}.$$

Compared to the isothermal compressible Navier-Stokes equation,

- $c_1 \neq c_2$ due to the lack of Galilean invariance;
- Instead of momentum conservation, there is the geometric constraint on Ω.

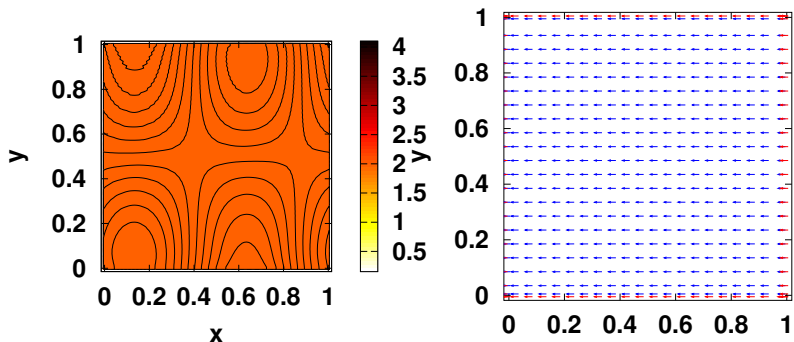Ref.: Generalized Collision Invariants (GCIs) by P. Degond and S. Motsch (2008).

We start with a biased random initial velocity field such that the self-organzation will move to the left.
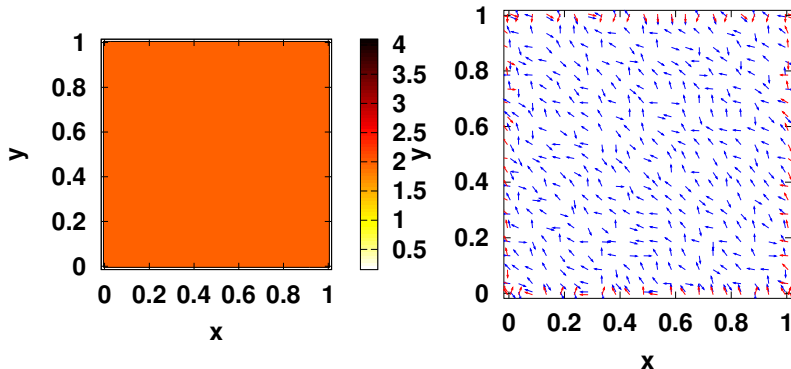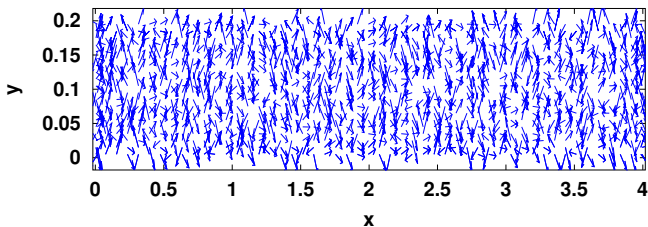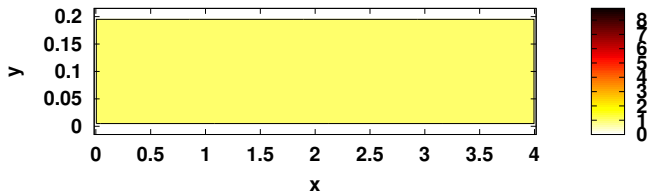
SOHR model in a square

After the global alignment is formed, instead of horizontal contours for the density distribution, small perturbation at the upper and lower boundaries occurs.
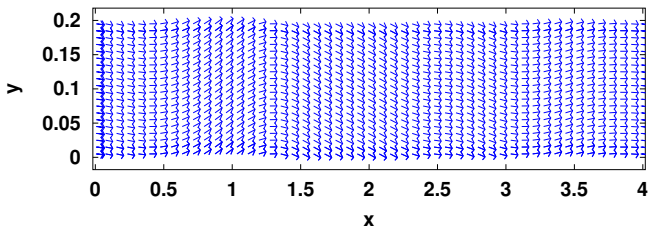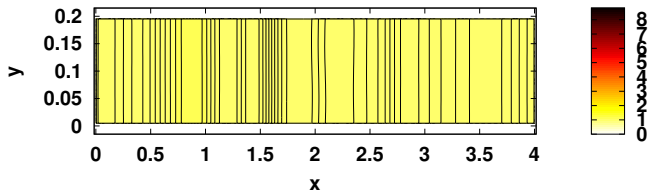
We start with a biased random initial velocity field such that the self-organization will move to the right.

YU, Hui   Boundary interaction for collection motion

After the global alignment is established, the velocity field wave between the upper and lower boundaries.

- The alignment frequency σ and the noise D_b at the boundary.

- The average density and the optimal speed of the self-organization.

- The application to the annular ring.

- ...